MOLECULAR AND CELLULAR BIOLOGY, Mar. 2007, p. 2398–2410 Vol. 27, No. 6
0270-7306/07/$08.00+0 doi:10.1128/MCB.01509-06

Mechanism of Histone H1-Stimulated Glucocorticoid Receptor DNA Binding In Vivo▽†

Sergey Belikov, Carolina Åstrand, and Örjan Wrange*

Department of Cell and Molecular Biology, Karolinska Institutet, SE-17177 Stockholm, Sweden

Received 14 August 2006/Returned for modification 23 October 2006/Accepted 20 December 2006

***Xenopus* oocytes lack somatic linker histone H1 but contain an oocyte-specific variant, B4. The glucocorticoid receptor (GR) inducible mouse mammary tumor virus (MMTV) promoter was reconstituted in *Xenopus* oocytes to address the effects of histone H1. The expression of *Xenopus* H1A (H1) via cytoplasmic mRNA injection resulted in H1 incorporation into in vivo assembled chromatin based on (i) the appearance of a chromatosome stop, (ii) the increased nucleosome repeat length (NRL), and (iii) H1-DNA binding assayed by chromatin immunoprecipitation (ChIP). The H1 effect on the NRL was saturable and hence represents H1-binding to a specific site. A subsaturating level of H1 enhanced the hormone-dependent binding of GR to the glucocorticoid response elements (GREs) and the hormone-dependent MMTV transcription while it reduced the access to DNA as revealed by micrococcal nuclease (MNase) analysis. These H1 effects were lost at higher levels of H1. ChIP and MNase analysis revealed a hormone-dependent dissociation of H1 from the activated chromatin domain. The proposed mechanism of H1-induced GR binding is based on two effects: (i) a GR-induced asymmetric distribution of H1 in favor of inactive chromatin and (ii) an H1-induced reduction in DNA access. These effects results in increased concentration of free GR and, hence, in increased GR-GRE binding.**

The intranuclear DNA in the eukaryotic cell is organized into chromatin which consists of nucleosomes connected by ~20 to 80 bp of linker DNA (16, 43, 47). The length and structure of this linker DNA is modulated by linker histone H1, a protein family that is present in essentially all eukaryotes. Previous quantification of cellular H1 content suggested the presence of about one H1 molecule per nucleosome, i.e., an H1/N ratio of ~1. However, recent work has shown that linker histone/N ratios may vary from ~0.5 in embryonic cells to ~0.8 in several different cell types (47) and even up to ~1.3 in chicken erythrocytes (3). Histone H1 binds asymmetrically to nucleosomal DNA without any known sequence specificity, the DNA interaction occurs simultaneously near the nucleosomal dyad (43) and the linker DNA (14, 48). In mice, for example, there are at least eight H1 subtypes that differ in amino acid sequence and expression during different stages of development and in different cell types (reference 20 and references therein).

The incorporation of histone H1 into in vitro-reconstituted chromatin has demonstrated its ability to stabilize the higher-order chromatin structure (25, 26), to reduce nucleosome sliding (4, 45) as well as to reduce DNA access, and thus, to act as a global repressor for basal or nonspecific transcription (29). Chromatin reconstitution of the hormone-inducible mouse mammary tumor virus (MMTV) promoter in *Drosophila* embryo extracts showed histone H1 to enhance progesterone receptor (PR) binding to DNA and to selectively promote the synergistic effect on transcription mediated by the nuclear factor 1 (NF1) and PR (28). The authors proposed that the H1-enhanced PR binding was due to the DNA sequence dependent nucleosome structure of the MMTV promoter.

In vivo studies where the histone H1 gene was deleted in *Tetrahymena* and in *Saccharomyces cerevisiae* demonstrated it to be nonessential and to cause only minor effects on transcription (reference 47 and references therein). Remarkably, the removal of one or two of five somatic linker histone variants in the mouse did not result in any effect on the phenotype but was compensated for by the increased expression of the remaining H1 subtypes. However, the concomitant deletion of three H1 subtypes resulted in embryonic lethality (19). The analysis of cells derived from such embryos revealed an ~50% reduction in the total histone H1 content, a reduction of the nucleosome repeat length (NRL) by ~8 bp to 15 bp, and an altered gene expression, some transcripts were increased and others decreased (19, 20).

Pioneering chromatin immunoprecipitation (ChIP) experiments in tissue culture cells demonstrated a reduced binding of linker histone H1 in the hormone-activated MMTV promoter (11). Similar findings were obtained in in vivo and in vitro assembled MMTV chromatin (23, 28). The overexpression of histone H1 in tissue culture cells already containing endogenous H1 caused a 1.2- to 1.4-fold increase in total H1 and enhanced both basal transcription and glucocorticoid hormone-dependent transcription from the stably integrated MMTV promoter. These effects were not observed in transiently transfected MMTV-driven reporters (24). The mechanism of this H1-mediated enhancement of MMTV transcription in vivo has, however, remained unresolved (13).

Oocytes from the frog *Xenopus laevis* were shown to be useful for studies of a variety of cellular processes (12), including the regulation of heterologous genes (32, 38). We have demonstrated that the MMTV long terminal repeat (LTR), after in vivo chromatin assembly in *Xenopus* oocytes, shows the

* Corresponding author. Mailing address: Dept. of Cell and Molecular Biology, The Medical Nobel Institute, Box 285 Karolinska Institutet, SE-17177 Stockholm, Sweden. Phone: 46 8 5248 7373. Fax: 46 8 313529. E-mail: orjan.wrange@ki.se.

† Supplemental material for this article may be found at http://mcb.asm.org/.

▽ Published ahead of print on 8 January 2007.

same characteristics as when stably integrated in tissue culture cells in terms of the hormone regulation, the chromatin organization, and the factor binding (8). Incidentally, *Xenopus* oocytes as well as early embryos are deficient in somatic histone H1 but contain an oocyte-specific maternal linker histone variant called B4, also known as H1M (18). After the midblastula transition, histone B4 is progressively substituted for somatic histone H1 variants, predominantly H1A (37). Likewise, mouse oocytes lack somatic linker histones but contain an oocyte-specific variant, histone H1oo (42). Photobleaching experiments utilizing H1-green fluorescent protein fusion proteins revealed H1 to be mobile (30, 33). This implies that heterologously expressed H1 may be able to bind to chromatin assembled in *Xenopus* oocytes. Based on this assumption and on the lack of somatic linker histones, *Xenopus* oocytes offer a unique potential to address various mechanistic aspects of H1-mediated effects on chromatin structure and gene induction.

Below, we demonstrate that *Xenopus* histone H1A, from here on dubbed H1, is incorporated into in vivo assembled chromatin and induces an 9- to 12-bp increase of the NRL. We demonstrate that this H1-mediated effect is saturable and, hence, represents H1 binding to a specific site in chromatin. The specific H1 binding was not reduced by overexpression of the oocyte-specific linker histone B4. This provided the opportunity to monitor the H1-induced effect on GR binding and MMTV transcription in vivo and chromatin structure in situ without detectable influence of endogenous linker histone(s). Such experiments demonstrated that a subsaturating concentration of H1 enhances the DNA binding of hormone-activated GR as well as hormone-induced MMTV transcription, and in addition, this same H1 concentration induces a reduced DNA access based on micrococcal nuclease (MNase) digestion in situ. All of these H1 effects are gradually lost as the H1 concentration is increased. These observations converge into a mechanism of H1-stimulated GR binding that may be of general functional significance.

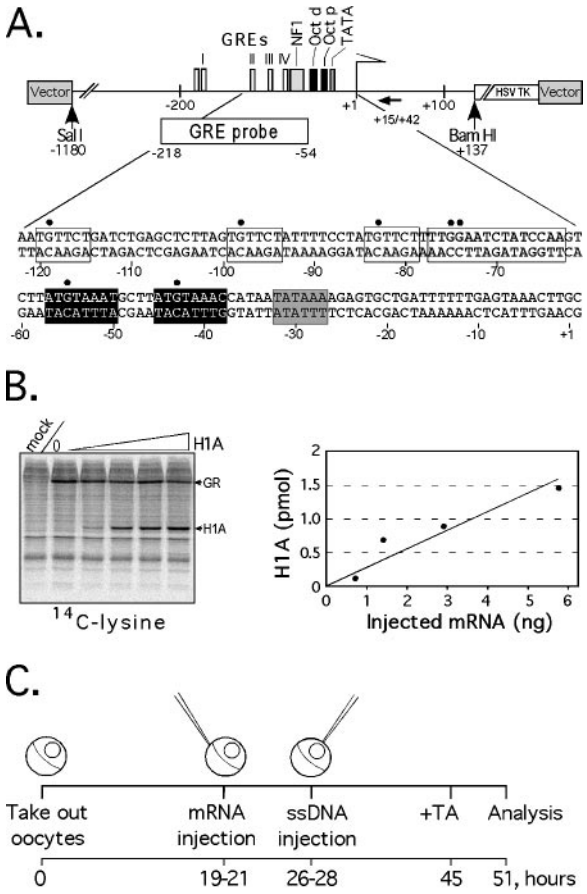

FIG. 1. (A) The MMTV reporter construct pMMTV:M13. The black arrow indicates the primer used for DMS methylation protection. Black dots show protected guanines in DMS in vivo footprinting. The GRE probe (−218/−54) was used in MNase experiments. (B) Estimation of intranuclear H1A content. Autoradiography of SDS-PAGE of *Xenopus* oocyte nuclear extract after injection of 0, 0.7, 1.4, 2.9, and 5.8 ng of H1 mRNA and 4 ng of GR mRNA and incubation with 3 μCi/ml of [^{14}C]lysine. Right: translated H1A protein is plotted versus injected mRNA as quantified by comparison to GR standard. (C) The experimental design followed unless otherwise indicated. This protocol generated an H1/N ratio of ~1 when injecting 0.27 ng H1A mRNA and 3 ng ssDNA.

MATERIALS AND METHODS

Plasmids. The DNA construct referred to as the MMTV reporter DNA is pMMTV:M13 (6). The construction of the plasmids for in vitro production of mRNA for rat glucocorticoid receptor (GR) (6), pig NF1-C1 (NF1), and human Oct 1 (Oct1) has been described previously (5). The plasmids for production of mRNA for *Xenopus laevis* histone H1A were from a PCR-amplified xH1A cDNA clone (a generous gift from K. Oshumi, accession no. DQ466082), and those for *Xenopus laevis* maternal linker histone were from a PCR-amplified B4 cDNA clone (a generous gift from K. Ura, accession no. L22845). The double hemagglutinin (HA) tag was generated from PCR amplification of plasmid pB2385 (a generous gift from Per Ljungdahl, The Ludwig Institute, Stockholm) with primers 5′-GAGAGGATCCACAGCCACCATGTACCCATACGATGTTCTTGAC TAT-3′ and 5′-GAGAGAGATCTTGCATAGTCCGGGACGTCATAGGG-3′. The PCR product and RN3P vector containing the xH1A clone described above were cut with BamHI and BglII before ligation to the N-terminal domain of xH1A. The pGo2.5Go-39MTV:M13 construct utilized the 20-bp TG-repeat DNA bending sequence (40) and two glucocorticoid response elements (GREs) with their major grooves for GR binding facing out, i.e., the periphery of the curvature as described before (31) and illustrated in Supplement S1 in the supplemental material.

Oocyte injections. Oocyte injections were carried out as described earlier (6). The synthetic glucocorticoid hormone, triamcinolone acetonide (TA), was added to the oocyte medium at a 1 μM concentration or as indicated. The 3 ng of circular single-stranded (ss) M13 DNA was injected into the oocyte nucleus resulting in ~6 ng of double-stranded DNA (dsDNA) after second-strand synthesis occurring within 3 to 4 h after injection (1). Quantification of injected DNA recovered in 16 pools of 9 oocytes each by primer extension showed a variation in the DNA recovery with a standard deviation of ±32%. For each analysis, 2 to 3 pools of oocytes were injected and independently analyzed to control for experimental variability. The results are indicated by two black dots in the diagrams and the average result as a bar (double samples) or by error bars for standard deviations (triplicates).

Quantification of expressed H1 protein. Quantification of expressed H1 protein was done after sodium dodecyl sulfate-polyacrylamide gel electrophoresis (SDS-PAGE) analysis of nuclei isolated from injected oocytes by relating the incorporated radioactivity of the in vivo [^{14}C]lysine-labeled H1 band to that of the ~90-kDa GR protein band obtained after injection of an mRNA mix coding for GR and H1 and correcting for their different numbers of lysine residues. The absolute amount of GR in the oocyte nucleus was estimated by Western blot analysis using a standard curve of known amounts of purified GR (5), and this was then used to calculate the absolute amount of nuclear H1 by comparison to the radioactivity in the GR band (Fig. 1B).

Quantification of MMTV transcription. Quantification of MMTV transcription by S1 nuclease and DNA analysis have been described earlier (5). Double or triplicate samples of individual pools of the indicated numbers of oocytes were analyzed. No reference promoter could be used as an internal control, since its transcription is inhibited by the massive induction of the MMTV promoter upon hormone activation (5).

DMS in vivo footprinting and primer extension has been described previously (7).

Chromatin structure analysis. MNase digestion (6) and a supercoiling assay (7) were done as described previously, in the latter case, with a chloroquine concentration of 80 μg/ml in the agarose gel. After blotting and hybridization, the ^{32}P radioactivity scans and quantifications were done with a Fuji Bio-Imaging analyzer BAS-2500 using the Image Gauge V3.3 software. The maximum amplitude of the DNA topoisomer distribution was defined as the midpoint of the integrated surface under the radioactively labeled topoisomers. In indicated experiments, the 3 ng of ssDNA was coinjected with 90 nCi of [α-^{33}P]dCTP (~2,500 Ci/mmol) to in vivo label the DNA during second-strand synthesis, hence, allowing direct analysis of MNase ladders by PhosphorImager analysis of dried agarose gels (22).

ChIP. Histone HA-H1A, dubbed HA-H1, was immunoprecipitated in duplicate, as described previously (2), overnight with anti-HA antibody (Roche) on salmon sperm DNA-protein A-agarose beads (Upstate Biotechnology). The DNA was analyzed by quantitative PCR by SYBR green on an ABI PRISM 7000 Sequence Detection System (Applied Biosystems) with amplicons covering the B-nucleosome (−187/−96), thymidine kinase (TK) reporter gene (+476/+551), and M13 vector (~−4.1/−4.2 kb). All experimental values were normalized to the input.

RESULTS

Linker histone H1 expressed in *Xenopus* oocytes is incorporated into chromatin. The MMTV LTR harbors a cluster of at least four GR-binding sites, GRE I to IV (Fig. 1A), one homodimeric NF1-binding site, and two octamer factor-binding sites. The MMTV LTR mediates GR-driven transcription of the herpes simplex virus TK reporter gene (15) and was inserted into the filamentous phage M13 mp9 vector (6). The circular ssDNA was used for intranuclear injection into *Xenopus* oocytes, leading to second-strand DNA synthesis and chromatin assembly (1). *Xenopus* oocytes may be programmed to produce proteins at will in up to pmol amounts by injection of the corresponding in vitro-transcribed mRNA. Protein synthesis was monitored by incorporation of [^{14}C]lysine and SDS-PAGE (Fig. 1B). The amount of expressed H1 protein was quantified by relating it to a known amount of ~90-kDa GR protein as described in Materials and Methods.

In a typical experiment, the oocytes were first given a cytosolic injection with indicated mixes of mRNA, and 6 to 8 h later, an intranuclear injection of 3 ng MMTV reporter ssDNA, resulting in ~6 ng of intranuclear dsDNA (Fig. 1C). The analyses of the protein and DNA amounts were used to estimate the apparent linker histone H1 to nucleosome (H1/N) ratio. Our 10.25-kb DNA construct organizes 59 to 62 nucleosomes based on NRL of 164 and 173 bp in the absence or presence of histone H1, respectively (Fig. 2B; see also Fig. 4B). The ~6 ng of recovered reporter dsDNA infers that these oocytes contain on the average ~0.05 pmol of nucleosomes at an NRL of 173 bp (Fig. 2C). The endogenous oocyte DNA is ignored, since it represents only ~0.6% of the total nuclear DNA. Two independent titration experiments with H1 mRNA revealed similar quantitative results (Fig. 1B and data not shown). From the linear titration curves, we calculated that the injection of 0.35 ng and 0.7 ng of H1 mRNA resulted in ~65 fmol and ~130 fmol of nuclear H1 protein, respectively, at ~32 h after mRNA injection. This renders the apparent intranuclear H1/N ratios of ~1.3 and ~2.6, respectively. All H1/N ratios given in the following experiments were based on these quantifications. Note that this H1/N ratio is based on the total nuclear histone H1, i.e., the sum of the fraction of H1 appropriately bound to chromatin, the free pool, and the nonspecifically bound H1. Furthermore, the individual variability of the DNA amount recovered after intranuclear injection in individual oocytes made it necessary to analyze pools of oocytes. Taken together, the apparent H1/N ratio thus offers only a crude estimation of the average amount of intranuclear H1 that was present in relation to the DNA in each pool of oocytes.

The binding of linker histone H1 to the nucleosome dyad and to the linker DNA in the chromatin fiber is known to generate a weak and transient chromatosome stop of about 165 bp, as revealed by MNase digestion. Further digestion generates the 145-bp nucleosome core particle (43). We analyzed the in situ MNase digestion pattern of the electrophoretically separated mononucleosomes from injected oocytes (Fig. 2A). At the lowest MNase concentration, we observed a smear extending from 150 bp to 190 bp (compare lanes 1 in Fig. 2A), while the highest MNase concentration revealed the 145-bp nucleosome core particle (Fig. 2A, lanes 3 and scan). At an intermediate concentration of MNase, there was an H1-dependent appearance of two merged bands of a nucleosome core fragment and a chromatosome fragment of ~145 bp and 165 bp, respectively (Fig. 2A, compare lanes 2 and scans). Digestion profiles and corresponding scans of H1-containing chromatin under mild MNase digestion conditions revealed a similar pattern when H1 mRNA was administrated to reach an apparent H1/N ratio from ~1.3 to 8.3, arguing for the formation of a similar chromatosome particle even at some excess of H1. The MNase ladder was less distinct, and the chromatosome stop was not resolved when a large excess of H1 was expressed to achieve an apparent H1/N ratio of 52 (Fig. 2A). This probably reflects nonspecific binding of H1 to DNA which compromises the chromatin structure and the MNase digestion at the highest H1 concentration.

The MMTV LTR is constitutively organized into six translationally positioned nucleosomes in tissue culture cells (35, 44), and we showed a similar arrangement to occur in the MMTV LTR in *Xenopus* oocytes upon hormone induction (6). Two experiments based on hydroxyl radical footprinting and MNase digestion followed by analysis with Southern blotting and indirect end labeling as described before (6) did not reveal any significant H1 effect on the translational nucleosome positioning neither in inactive nor in the hormone-activated MMTV LTR (data not shown).

Histone H1 incorporation results in a saturable increase of the NRL. Previous studies have demonstrated that incorporation of linker histones into chromatin causes an increase in the NRL both in vivo (24, 47) and in vitro (21). In our hands, all pools of H1 containing *Xenopus* oocytes with an apparent H1/N ratio of ~1.6 or more displayed an increase in the NRL of 9 bp to 12 bp (Fig. 2B and C; see also Fig. 4B). The H1-induced increase in NRL was affected by the temperature and the extent of MNase digestion. This is probably caused by nucleosome sliding during MNase digestion which tends to reduce the NRL (9). To minimize this effect, we reduced the temperature during MNase digestion from 25°C to 15°C. Plots of nucleosome ladder number versus NRL showed a linear relationship and rendered an NRL for control chromatin of ~164 bp. Incorporation of histone H1 at an apparent H1/N ratio of ~2 increased the NRL to ~173 bp and in some experiments up to 176 bp (Fig. 2C; see also Fig. 4B). Interest-

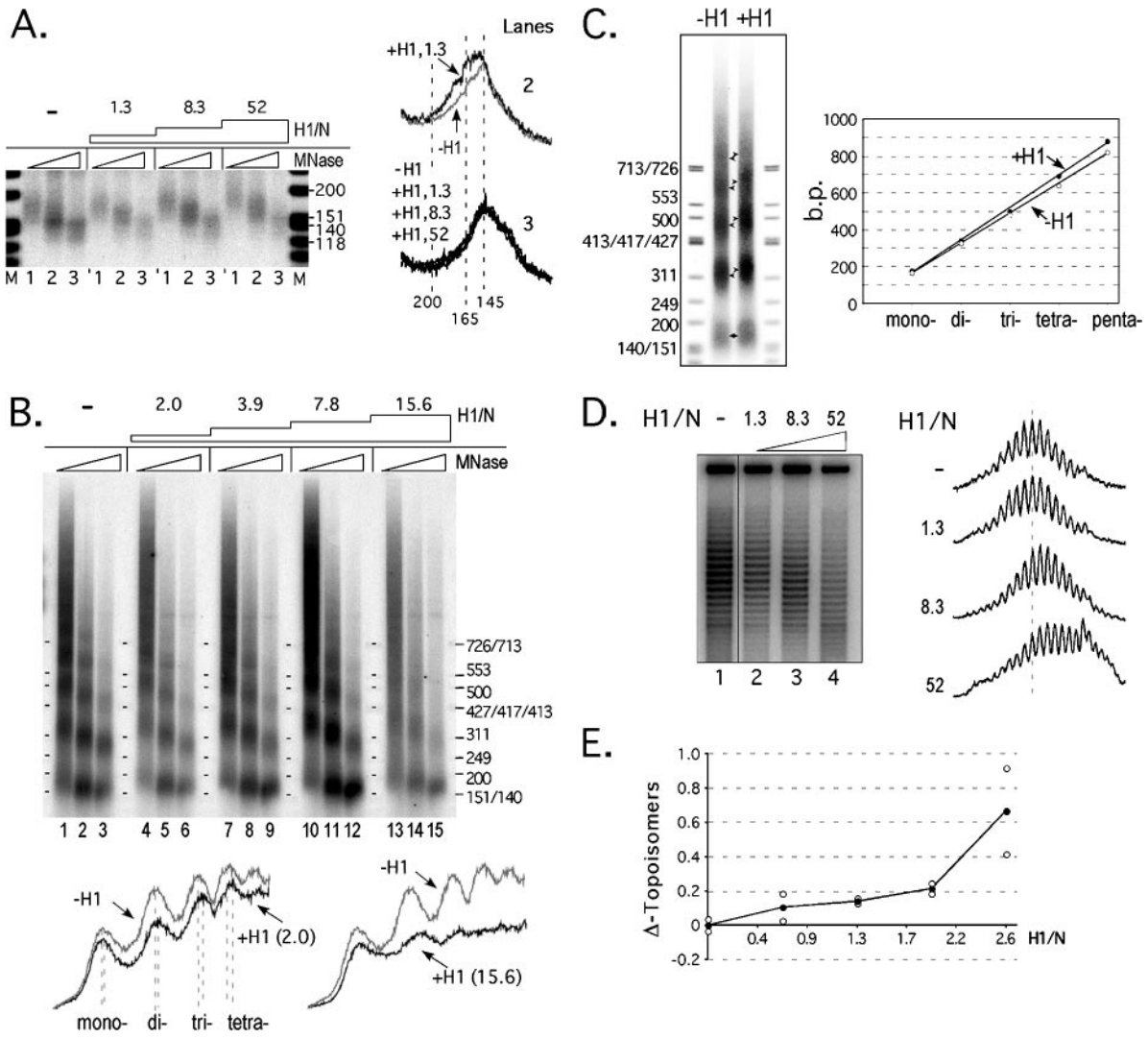

FIG. 2. (A) An H1-dependent chromatosome stop is detected by MNase digestion. Groups of 10 oocytes were injected with H1 mRNA as illustrated in Fig. 1C. Oocyte homogenate was digested with MNase (5, 15, and 45 U in lanes 1, 2, and 3, respectively, at 25°C for 5 min). DNA was resolved in a 3.6% agarose gel and hybridized with ^{32}P-labeled pMMTV:M13 DNA. Scans of lanes 2 and 3 are shown to the right with stippled lines for calculated sizes (in bp). (B) Effect of histone H1 on NRL. The procedure was the same as described for panel A but with the injection of 4 ng ssDNA and using a 1.6% agarose gel. Scans of lane 1 versus lane 4 and lane 1 versus lane 13 are shown. (C) Effect of histone H1 on NRL at low temperature. The procedure was the same as described for panel A but with H1 mRNA injected to achieve an H1/N ratio of ~1.3 and digestion of 9 U MNase at 15°C for 5 min. Arrowheads mark the MNase ladders. Right: plot of DNA length versus nucleosome number. Open and black circles show the data points for without and with H1 chromatin (−H1 and +H1), respectively. The lines show linear regressions which indicate NRLs of ~164 and ~176 bp for −H1 and +H1 chromatin, respectively. (D) Effect of H1 on DNA topology. Injections were as described for panel A and illustrated in Fig. 1C but using 3 ng ssM13mp18. DNA was separated on a 1% agarose gel. Right: profiles of scanned lanes show the distributions of topoisomers, and the stippled line indicates the midpoint for cells without H1. (E) An H1-induced transition in topology effect at an H1/N ratio of ~2.6. The procedure was the same as described for panel D but with double samples of pools of 10 oocytes (open circles) and average values (black dots).

ingly, the MNase digestion pattern and NRLs were constant within a wide range of apparent H1/N ratios from ~2 to 8 (Fig. 2B, compare lanes 4 to 6, 7 to 9, and 10 to 12). However, when the H1/N ratio reached ~16 (Fig. 2B, lanes 13 to 15 and scan below), the typical nucleosome ladder faded and was partially replaced by a smear, probably due to aberrant binding of H1 (see Discussion and Supplement S3 in the supplemental material).

Topological analysis of the injected circular M13 DNA showed an increasing loss of ~2 and ~4 negative supercoils when the apparent H1/N ratio was increased to 8.3 and 52, respectively (Fig. 2D). This indicates either a loss of an equal number of nucleosomes or an altered linker DNA structure (41). In either case, such high levels of H1 have significant effects on the chromatin structure, as revealed by a smearing effect on the MNase ladder (Fig. 2B). However, an H1-induced increase of the NRL by 9 to 12 bp was seen already at an apparent H1/N ratio of 1.6 to 2 (see Fig. 4B) where no significant effect on the topology was observed (Fig. 2E). A titration of increasing amounts of H1 in small steps again revealed no

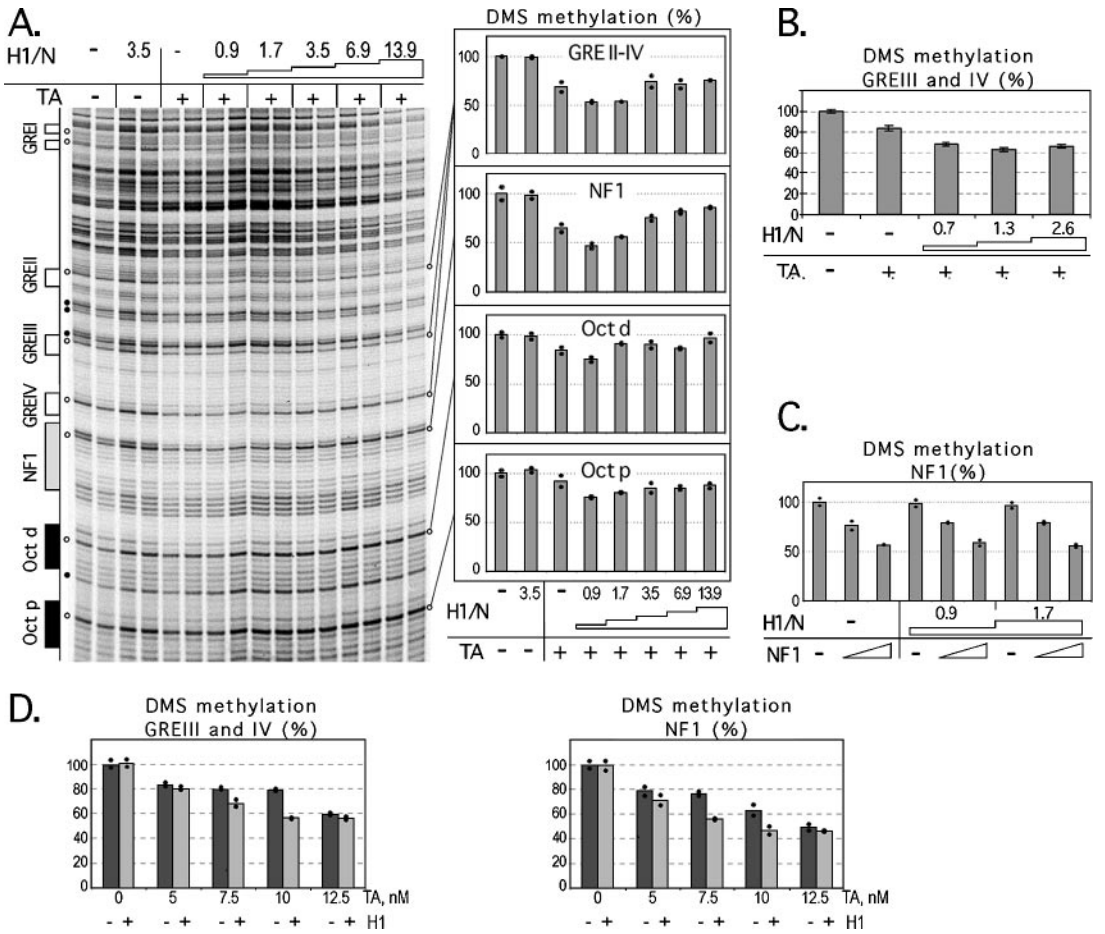

FIG. 3. (A) Binding of GR, NF1, and Oct 1 to hormone-activated MMTV promoter is enhanced at an apparent H1/N ratio of ~1. DMS methylation protection analysis of oocytes injected as illustrated in Fig. 1C with mRNA mixes to achieve the indicated H1/N ratios and containing 3.68, 0.76, and 3.22 ng per oocyte of GR, NF1, and Oct1 mRNAs, respectively, is shown. Duplicate pools of eight oocytes were analyzed. Methylation protection of indicated bands (open circles) was quantified and related to the sum of indicated reference bands (black dots), with the absence of hormone level (−TA) set to 100%. Right: diagrams of DMS methylation; black dots are individual samples and bars are mean values. (B) Binding of GR in the absence of NF1 and Oct1 is enhanced at an apparent H1/N ratio of ~1. DMS methylation protection analysis of triplicate pools of eight oocytes was as illustrated in Fig. 1C and described for panel A but used 2.8 ng of GR mRNA. The results in the diagrams are the averages of triplicates with standard deviations shown as error bars. (C) Constitutive binding of NF1 to the inactive MMTV promoter is not affected by an apparent H1/N ratio of 1 to 2. DMS methylation protection analysis of duplicate pools of eight oocytes injected and assayed as described for panel A but with 2.1 ng GR mRNA and increasing amounts of NF1 and Oct1 mRNAs, i.e., 0, 0.23, and 1.4 ng NF1 and 0, 1.6, and 6.7 ng of Oct1 mRNA per oocyte, respectively. No hormone was added. (D) The H1-dependent enhancement of GR binding is more prominent at low glucocorticoid hormone concentration. DMS methylation protection analysis of duplicate pools of eight oocytes was as described for panel A but with an mRNA mix for GR, NF1, and Oct1 mRNA of 3.9, 0.39, and 3.7 ng, respectively, in the absence (−, dark gray bars) or presence (+, light gray bars) of 0.35 ng H1 mRNA to generate an H1/N ratio of ~1.3. Hormone (TA) was added at the concentrations indicated.

major change in DNA topology up to an apparent H1/N ratio of ~2 and then a significant loss of negative supercoiling at an H1/N ratio of ~2.6 and above (Fig. 2E and data not shown).

We conclude that (i) increasing levels of H1 correlate with a gradually increased NRL up to ~9 to 12 bp, (ii) the H1-dependent increase in NRL is saturable, and (iii) this H1-induced effect on the NRL occurs without any major change in DNA topology.

Linker histone H1 enhances hormone-induced binding of GR to its cognate DNA sites. The sequence-specific binding of proteins to DNA was monitored in vivo by dimethylsulfate (DMS) methylation protection (7). We quantified GR, NF1, and Oct1 binding at the MMTV LTR in the presence of increasing intranuclear concentrations of histone H1 and in the presence or absence of glucocorticoid hormone (TA). Hormone activation resulted in a drastic reduction of the DMS methylation over the GRE II-IV and NF1 binding sites to average values of 68% and 65% methylation, respectively, compared to the DMS methylation in the absence of hormone defined as 100%. There was also a weak methylation protection over the distal and proximal Oct sites (Fig. 3A) (8). Unexpectedly, the expression of linker histone at an apparent H1/N ratio of ~1 rendered a further reduction in DMS methylation to give average values of 54%, 47%, 75%, and 76% for GREs, NF1 site, Oct d, and Oct p, respectively. Thus, the H1-dependent ~1.5-fold reduction in methylation of the binding sites reflected a corresponding H1-dependent increased binding of GR, NF1, and Oct1 to their cognate DNA sites. This

H1-dependent effect was only seen in the presence of glucocorticoid hormone (Fig. 3A) and was dependent on the injection of the mRNA coding for these factors (8; data not shown); the pattern of methylation protection was confined to their cognate factor binding sites. An additional increase in H1 content to an apparent H1/N ratio of ~4 resulted in the loss of the H1 stimulatory effect for all three factors. Even higher H1 levels led to gradual inhibition of NF1 and Oct1 binding while GR binding remained at the level obtained in the absence of H1 (Fig. 3A).

We conclude that an apparent linker histone H1/N ratio of ~1 renders an increased binding of GR, NF1, and Oct1 at the hormone-activated MMTV LTR and that this effect is reduced by a 2-fold increase and completely lost already at an ~4-fold increase of the H1 content (Fig. 3A). Since we have previously shown that GR, NF1, and Oct1 bind cooperatively to the hormone-activated MMTV LTR (8), we also evaluated the effect of H1 on the hormone-dependent GR binding in the absence of NF1 and Oct1. Here, the addition of hormone resulted in the reduction of DMS methylation from 100% ± 1% to 83 ± 2%. The level of H1 providing an apparent H1/N ratio of ~1.3 showed maximal reduction in GRE-specific methylation from 83 ± 2% to 63 ± 2%, thus reflecting maximal stimulation of GR binding (Fig. 3B). Furthermore, we observed that all four GREs within the proximal MMTV LTR displayed a similar level of H1-dependent reduction of DMS methylation, i.e., stimulation of GR binding (data not shown).

We have previously shown that NF1 (5) and Oct1 (8) are constitutively and cooperatively bound to their specific sites in the MMTV promoter also in the absence of hormone, albeit to a low level compared to the hormone- and GR-dependent binding of NF1 and Oct1. This urged us to address the effect of histone H1 on this constitutive NF1 and Oct1 binding. Increasing amounts of mRNA coding for Oct1 and NF1 in the absence or presence of histone H1 mRNA rendering apparent H1/N ratios of 0, ~0.9, and ~1.7, respectively, were injected into oocytes and analyzed by DMS in vivo footprinting (Fig. 3C). The results show that histone H1 has no effect on NF1 (Fig. 3C) or on Oct1 methylation protection (data not shown). The expected levels of H1, NF1, and Oct1 were achieved as confirmed by SDS-PAGE analysis (data not shown). Furthermore, the previously described constitutive NF1- and Oct1-dependent MMTV transcription (5) was also detectable and was not affected by the presence of H1 (not shown). We conclude that it is only in the hormone-activated state that H1 stimulates specific protein-DNA interactions.

We then addressed whether H1-mediated stimulation of GR and NF1 binding would be stronger in relative terms at a lower level of GR induction. This was achieved by a stepwise increase of the glucocorticoid hormone, i.e., TA, added to the oocytes previously injected with GR, NF1, and Oct1 mRNA in the absence or presence of histone H1 mRNA to render an apparent H1/N ratio of ~1.5. DMS in vivo footprinting revealed an enhanced GR and NF1 binding in the presence of histone H1 (Fig. 3D). The most prominent H1-dependent stimulation of methylation protection, i.e., factor binding, was observed at 7.5 to 10 nM TA. This is the hormone concentration previously shown to render half-maximal GR-DNA binding and transcription (7). Furthermore, the GR and NF1 binding reached a plateau at a lower hormone concentration in the presence of H1 (Fig. 3D). We conclude that the H1-dependent stimulation of GR and NF1 binding is more prominent at a lower and perhaps more physiological concentration of hormone-activated GR.

Previous in vitro experiments on chromatin-reconstituted MMTV template in *Drosophila* embryo extracts demonstrated an increased synergistic effect of NF1 and PR on DNA binding and in vitro transcription by the addition of an ~1 H1/N ratio of linker histone H1 (28). Based on the lack of such an effect in a mutated MMTV construct, these authors suggested the special DNA sequence of the wild-type MMTV DNA to be the cause of this H1 effect. Since we also saw a stimulation of GR, NF1, and Oct1 binding in the presence of a balanced amount of H1, we decided to test whether this would occur for a GRE placed in a different DNA context and in the absence of NF1 and Oct1. To this end, we constructed the Go2.5Go DNA segment containing two GR binding sites positioned 80 bp apart within a synthetic DNA bending sequence, the TG-DNA sequence (40), which has a defined helical setting on an in vitro reconstituted nucleosome (see Supplement S1 in the supplemental material). The DMS in vivo footprint of this synthetic GRE in *Xenopus* oocytes revealed a similar degree of H1-dependent stimulation of GR binding as seen for the MMTV promoter (compare Fig. 3B and Supplement S1 in the supplemental material). This construct also displayed robust hormone-dependent transcription (unpublished result). We conclude that the H1-dependent enhancement of GR binding reported here is neither confined to the DNA sequence of the MMTV GRE nor dependent on the presence of NF1 and/or Oct1, as also indicated in Fig. 3B.

A subsaturating level of linker histone H1 concentration with respect to the effect on NRL enhances hormone-induced GR-DNA binding. The analysis of NRL by MNase digestion showed that the H1-dependent increase in the NRL was saturated at an apparent H1/N ratio of ~2 (Fig. 2B). Importantly, the DMS in vivo footprinting analysis revealed a bell-shaped curve of maximal H1-dependent stimulation of GR binding below this concentration of H1. To more carefully correlate these two events, we conducted the DMS in vivo footprinting analysis and the MNase-based analysis of the NRL in parallel. Pools of oocytes were injected with increasing amounts of H1 mRNA and an identical mRNA mix coding for GR, NF1, and Oct1. After mRNA injection, the oocytes were either injected with 3 ng of the single-stranded MMTV reporter DNA and used for DMS methylation protection analysis (Fig. 4A) or injected with the same amount of single-stranded MMTV reporter DNA and [α-^{33}P]dCTP to in vivo label the DNA for MNase digestion and analysis of the NRL (Fig. 4B and C). As shown in Fig. 3A, the DMS analysis of GR binding revealed a bell-shaped curve of H1-dependent stimulation of hormone-activated GR binding (Fig. 4A). A maximal stimulation of GR binding occurred at an H1 concentration of around half-maximal saturation, as defined by its effect on the NRL (Fig. 4, compare A and B), i.e., an apparent H1/N ratio of ~0.9, whereas the NRL reaches a plateau at an H1/N ratio of ~1.6 to 2.

We conclude that the enhanced GR-DNA binding occurs at a subsaturating intranuclear concentration of H1. The diagram describing the NRL as a function of the apparent H1/N ratio (Fig. 4B) can be used to estimate the fraction of nucleosomes

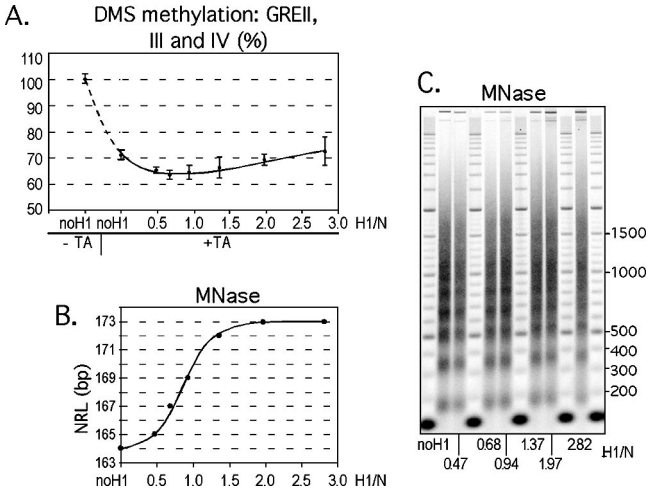

FIG. 4. Maximal H1-stimulated GR binding by DMS methylation protection analysis in vivo (A) occurs at half-maximal H1 binding to chromatin as defined by the H1-induced effect on NRL by MNase digestion in situ (B and C). Oocytes were injected and hormone treated as illustrated in Fig. 1C with mRNA mixes to achieve indicated H1/N ratios, i.e., 0, 0.11, 0.18, 0.25, 0.37, 0.56, and 0.76 ng H1 mRNA, and also containing 2.3, 0.35, and 1.8 ng per oocyte of GR, NF1, and Oct1 mRNAs, respectively, and then injected with 3 ng ssDNA MMTV reporter in the absence (A) or presence (B and C) of 90 nCi of [α-^{33}P]dCTP to in vivo label the DNA. Triplicate pools of 10 oocytes were analyzed by DMS methylation protection for each pool (A), and 100% methylation is defined by the DMS methylation in the absence of H1 and hormone (−TA, stippled line), while the black line describes the plot of apparent H1/N ratio versus GR binding monitored as methylation protection in the presence of hormone (+TA). The results in the diagrams are the averages of triplicates, with standard deviations indicated by error bars. (B) Ten oocytes from each pool without hormone treatment were taken for MNase analysis of the NRL. Isolated DNA was resolved in a 1.8% agarose gel. MNase ladders were visualized by PhosphorImager analysis of dried agarose gels.

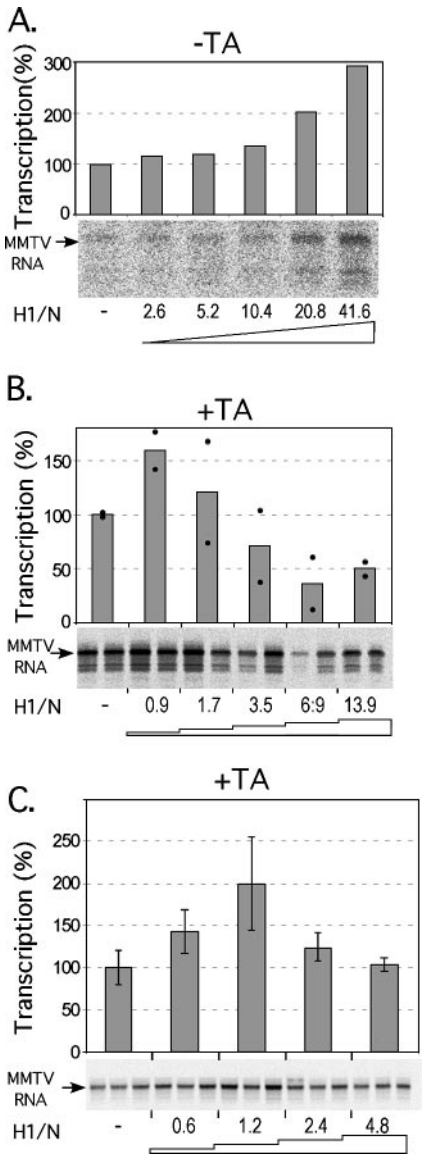

FIG. 5. (A) Histone H1 enhances basal MMTV transcription only at very high H1/N ratios. S1-nuclease analysis of MMTV-driven transcription of groups of 8 oocytes injected with 2.8 ng of GR mRNA and increasing amounts of H1 mRNA to achieve the apparent H1/N ratios indicated was done according to the procedures illustrated in Fig. 1C. No hormone was added (TA). (B) Hormone-activated MMTV transcription is enhanced at an apparent H1/N ratio of ~1 and is partially inhibited at higher levels. S1-nuclease analysis of MMTV transcription of duplicate pools of eight oocytes injected with mRNA mixes containing 3.7, 0.8, and 3.2 ng of GR, NF1, and Oct1 mRNA, respectively, and amounts of H1 mRNA to achieve the apparent H1/N ratios indicated was done according to the procedures illustrated in Fig. 1C. (C) An apparent H1/N ratio of ~1 enhances hormone-dependent MMTV transcription. The experiment was as described for Fig. 4B but used triplicate pools of eight oocytes and injection with mRNA mixes containing 1.2, 0.9, and 2.3 ng of GR, NF1, and Oct1 mRNA, respectively.

engaged in H1 binding at a given amount of total intranuclear H1, here expressed as the apparent H1/N ratio. This is based on the assumption that a saturable effect on the NRL is reached at the stoichiometry of specifically bound H1/N ratio of 1:1, as was previously demonstrated to be the case in vitro (21). In our experimental setup, a half-maximal effect is reached at an apparent H1/N ratio of ~0.9 (Fig. 4B), whereas saturation is reached at an apparent H1/N ratio of ~1.6 to 2 (see Discussion).

The H1 concentration that stimulates GR binding also stimulates hormone-activated transcription. The constitutive MMTV transcription is typically below 1% of the hormone-induced transcription (5) and was not affected by the presence of histone H1 in the apparent H1/N ratio of ~1 to 5. A further increase in the apparent H1/N ratio resulted in a gradually increased constitutive MMTV transcription (Fig. 5A). The fact that the MNase analysis demonstrated a perturbed nucleosome organization in the presence of a high amount of histone H1 (Fig. 2B, lanes 13 to 15) suggests that the increased basal MMTV transcription represents leakage due to corrupted chromatin structure, presumably caused by an aberrant H1 binding that generates a more open chromatin structure.

Hormone-induced MMTV transcription was stimulated by an apparent H1/N ratio of ~1. However, a further increase of the H1 concentration resulted in a loss of this stimulatory effect at an apparent H1/N ratio of 3 to 4 and an even further increase of the intranuclear H1 amount resulted in further inhibition of transcription (Fig. 5B). Although the level of

H1-dependent stimulation of MMTV transcription was variable, we consistently rendered a bell-shaped H1-dependent stimulation curve with a maximum at an apparent H1/N ratio of ~1 and then a gradual loss of this effect at two- to fourfold-higher concentrations of H1 (Fig. 5C). We conclude that there is a stimulation of hormone-induced MMTV transcription that correlates to the H1-dependent stimulation of GR binding to its specific DNA target. The basis for this stimulation of transcription is likely to be an increased frequency of initiation, since we have shown previously that the hormone-induced MMTV transcription correlates to GR binding and chromatin remodeling (6, 7).

Increased expression of embryonic linker histone B4 has no effect on the chromatin architecture, MMTV transcription, or histone H1 binding. *Xenopus* oocytes contain a large stockpile of the maternal oocyte-specific linker histone B4. To address the effect of B4 on the MMTV reporter system, we increased the B4 protein content by injection of the corresponding mRNA into oocytes. Quantification of the B4 protein as described for Fig. 1B showed that the microinjection of 7 ng of B4 mRNA resulted in the expression of ~0.4 pmol B4 per oocyte nucleus. A Western blot based on a B4 antiserum showed that this represented a 2.7-fold increase in the B4 content compared to the endogenous level (Fig. 6A). This is equivalent to an apparent B4/N ratio of ~4.4 emanating from the endogenous stockpile and an apparent B4/N ratio of ~12 after expressing more B4 by the mRNA injection. The comparison of the hormone-induced MMTV transcription showed no significant difference between the oocytes with or without this excess of B4 (Fig. 6B). Furthermore, MNase analysis of nucleosome ladders did not reveal any difference in the absence or presence of the extra levels of B4 on the chromatin structure or on the NRL (data not shown).

A ChIP analysis was used to address the effect of B4 on the H1-DNA binding. Here we injected mRNA coding for an N-terminally HA-tagged H1 (HA-H1) which had the same capacity to increase the NRL (see Supplement S2 in the supplemental material) and to simulate GR binding to DNA (data not shown) as wild-type (wt) H1, thus demonstrating that it is incorporated correctly into chromatin. A ChIP experiment done in the context of a twofold increase in B4 content, i.e., with a B4/N ratio of ~8.8, showed no effect of B4 on the HA-H1 binding (Fig. 6C). However, the use of wt H1 as a competitor resulted in a drastic reduction in HA-H1 binding already at an ~1.7-fold excess of competitor (see Supplement S3 in the supplemental material). This indicates that B4, if at all bound to interphase chromatin, does not compete for the H1 binding site in chromatin in vivo. In line with this result, the analysis of linker histone binding to an in vitro-assembled dinucleosome by DNase I footprinting showed that the DNA linkers were protected by histone H1 but not by histone B4 (37). Together with our results, this suggests that linker histone B4 binds either very weakly or not at all to the chromatin-binding site of histone H1, and therefore, its overexpression has no effect on the structure and function of the MMTV promoter conditions used here. We cannot exclude that endogenous B4 may have an influence on our H1 titration experiments, but we find this to be unlikely based on the above results.

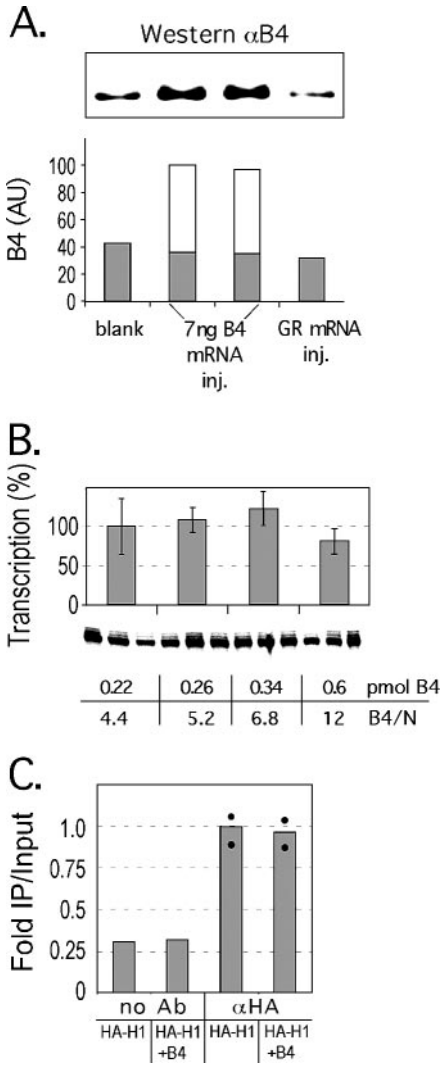

FIG. 6. Oocyte-specific linker histone B4 neither competes with H1 binding nor has an effect on the MMTV transcription. (A) Oocytes were injected (inj.) with the indicated amounts of B4 mRNA, and the increase in B4 content is shown by a Western blot probed with anti-B4 (αB4) on dissected nuclei, quantified below. (B) No effect on hormone-activated MMTV transcription was induced by an ~2.7-fold increase in histone B4. S1-nuclease analysis of MMTV transcription was carried out with triplicate pools of six oocytes injected with 1.8, 0.34, and 1.4 ng of GR, NF1, and Oct1 mRNA, respectively, and increasing amounts of B4 mRNA, followed by 3 ng of single-stranded pMMTV:M13 DNA to achieve the B4/N ratios indicated, estimated as shown in Fig. 1B. (C) ChIP analysis: B4 does not compete for H1 binding to chromatin. Oocytes injected with 0.6 ng HA-H1 mRNA to generate an ~1.3 H1/N ratio and with or without 3.9 ng B4 mRNA and 3 ng of single-stranded pMMTV:M13 DNA to render an apparent B4/N ratio of ~8.2. IP, immunoprecipitation.

Linker histone H1 is preferentially dissociated from the hormone-activated MMTV promoter and the transcribed TK reporter gene. *Xenopus* oocytes were injected with mRNA coding for GR, NF1, and Oct1 as well as for HA-H1 to render an apparent H1/N ratio of ~1.3, i.e., within the range that stimulates GR binding and used for ChIP. This revealed a robust H1-DNA cross-linking over the M13 vector, the MMTV promoter, and the TK gene in the absence of hormone induction

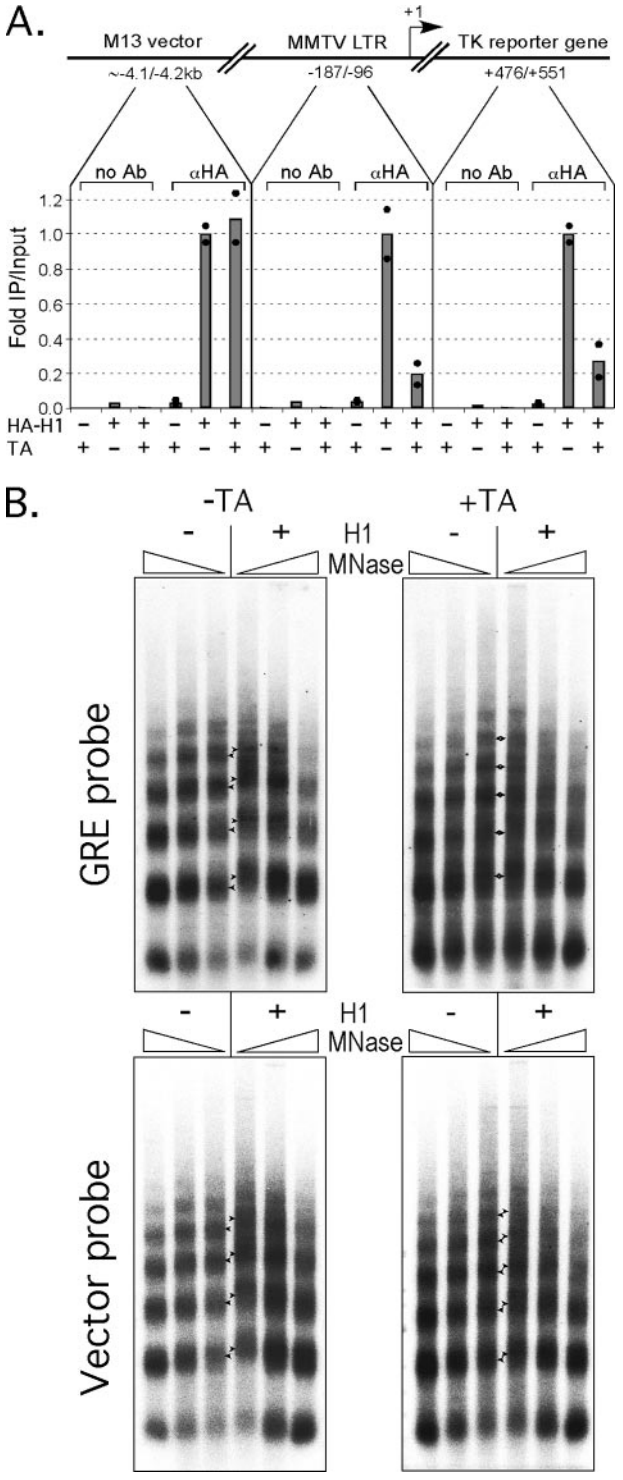

FIG. 7. (A) Histone H1 dissociates from the promoter and the transcribed region upon hormone activation. Oocytes were injected as described for Fig. 3A and with 0.6 ng of HA-H1 mRNA, followed by ChIP analysis in duplicate. The average amount of DNA relative to input (gray staples) precipitated for samples not treated with hormone was 1.25% at the promoter region, 1.34% at the TK reporter gene, and 0.57% at the vector region. These precipitated amounts were normalized to 1 in the diagram; black dots represent double samples of two independent immunoprecipitations (IPs). (B) Oocytes were injected with GR, NF1, and Oct1 mRNA mix as described for Fig. 3A and also with H1 mRNA to obtain an apparent H1/N ratio of ~1.3. Hormone treatment (TA) was as indicated: +, present; −, absent. For MNase digestion and analysis, see Fig. 3B. The filter was hybridized with ^{32}P-labeled GRE probe (Fig. 1A) and then, after stripping, rehybridized with ^{32}P-labeled M13 probe.

and a dramatic reduction in H1-DNA cross-linking in the promoter and transcribed gene after hormone induction (Fig. 7A). There was no reduction of H1 binding in the vector DNA.

The H1 contents of the MMTV promoter and the vector were also addressed by MNase digestion, followed by analysis of the NRL by consecutive hybridization with DNA probes for the MMTV GRE domain and for the M13 vector DNA (Fig. 7B). The H1-dependent increase in NRL was seen in absence of hormone in both DNA segments but was selectively lost in the GRE segment and surrounding area after hormone activation. This confirms the result of the ChIP experiment shown in Fig. 7A and demonstrates that there is a selective dissociation of H1 from the activated chromatin domain. We note that the hormone-induced loss of H1 cross-linking in active chromatin is not due to epitope masking, e.g., by H1 phosphorylation (10), since the antibody in our ChIP experiments recognizes the HA tag.

The hormone activation-dependent reduction in histone H1 binding at the MMTV promoter is in agreement with previous in vivo experiments using the MMTV promoter in tissue culture cells (11, 23). This suggests that the behavior of heterologously expressed H1 at the MMTV LTR in chromatin of *Xenopus* oocytes is similar to its behavior in other cells.

A subsaturating level of H1 reduces DNA linker access in situ, as revealed by MNase digestion. The ability of H1 to increase specific binding of GR, NF1, and Oct1 during hormone induction (Fig. 3) might be indirect, since it is implied by the ChIP and MNase analysis that H1 is dissociated from the MMTV promoter and the transcribed gene during hormone induction (Fig. 7A and B). Others have reported that a 1.2- to 1.4-fold overexpression of different H1 variants in tissue culture cells resulted in increased resistance of DNA to MNase digestion (24). We decided to address the effect of H1 expression on MNase digestion in our system in an effort to monitor the overall DNA accessibility as a function of H1 concentration. Hence, we conducted MNase digestion experiments after injection of increasing amounts of H1 mRNA and 3 ng of M13 ssDNA into oocytes. After MNase digestion, the isolated DNAs were restricted with BglII and HindIII to generate a 718-bp DNA fragment that was then quantified by Southern blotting and plotted as DNA protection (MNase cleaved/uncleaved DNA) as a function of the apparent histone H1/N ratio. Unexpectedly, this resulted in a bell-shaped curve of reduced MNase digestion at an apparent H1/N ratio of 1.0 to 1.3 (Fig. 8), i.e., at the same subsaturating level of H1 that enhances GR binding (Fig. 3) and MMTV transcription (Fig. 5). The H1-dependent protection from MNase digestion was 1.35-fold and was indeed significant, as judged from double samples and from yet another experiment reproducing this result both in terms of extent of protection and the H1 concentration at which it was achieved. Since MNase primarily attacks linker DNA, this result implies that a distinct alteration in linker DNA structure occurs at a rather narrow subsaturat-

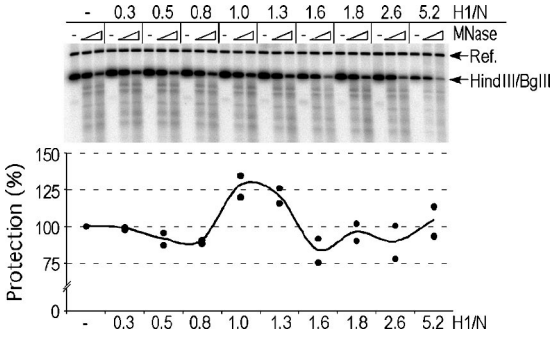

FIG. 8. Chromatin is more resistant to MNase in situ digestion at an H1/N ratio of ~1 to 1.3. Pools of 15 oocytes were injected as illustrated in Fig. 1C with H1 mRNA to achieve the indicated H1/N ratio and with 3 ng of single-stranded M13 mp18 DNA. The oocyte homogenates were subsequently digested with 0, 1.9, and 3.8 U of MNase at 18°C for 5 min. Stop mix with an 882-bp ^{33}P-labeled PCR fragment was added to each sample and served as an internal standard (Ref.). Isolated DNA was digested with HindIII/BglII to generate a 720-bp DNA fragment. This was resolved on a 1.6% agarose gel, transferred, and hybridized with ^{32}P-labeled HindIII/BglII M13 fragment. Protection is defined as digested HindIII/BglII fragment/nondigested (%), where −H1 oocyte pools were normalized to 100%. Black dots represent the two concentrations of MNase digestion.

ing level of H1. The structural changes involved in this H1 effect remain to be determined, but the fact that they occur at the same H1 concentration as the enhanced GR binding and MMTV transcription is quite striking and suggests a functional connection between these phenomena.

DISCUSSION

To the best of our knowledge, this is the first report to show that somatic linker histone H1 at a narrow concentration range enhances sequence-specific DNA binding of a gene regulatory protein in vivo. A prerequisite for this finding was the ability to express controlled amounts of somatic H1 in cells that lack endogenous H1, a criterion that is met by *Xenopus* oocytes but disqualifies many other cellular systems. Our titration experiments revealed that the H1-induced increase of the NRL is saturable and that maximal stimulation of GR binding occurred at a half-maximal saturation of H1-induced increase of the NRL (Fig. 4A and B), an H1 concentration that also induced an altered higher-order chromatin structure characterized by a reduced access of linker DNA (Fig. 8).

A saturable binding of H1 to chromatin in vivo. The structure of the chromatosome remains to be determined in full detail, but in vitro binding experiments (21, 26, 34) show that there is one high-affinity binding site of linker histone H1 or H5 per nucleosome. Importantly, Fyodorov and Kadonaga demonstrated a saturation curve showing that the NRL reaches a plateau at an H1/N ratio of ~1. Our results show, probably for the first time, that the H1 effect on the NRL is indeed saturable also in vivo. Others have suggested that the variation in NRL with H1 content is consistent with the maintenance of electrostatic charge homeostasis (47). Our result corroborates this view as long as the histone H1 content is below the level of saturation and until the preferred and specific binding site for H1 is saturated (Fig. 4B).

We do not interpret the saturation of the H1-induced NRL at an apparent H1/N ratio of ~1.6 to 2 found here (Fig. 4B) as an argument for more than one specific binding site of H1 per nucleosome. The reason is that we are measuring the total H1 in microdissected oocyte nuclei, i.e., the sum of specifically bound, free, and nonspecifically bound H1. It is conceivable that an excess of intranuclear H1 is required to saturate the specific chromatin sites, especially so in the giant nucleus of the *Xenopus* oocyte that harbors a large stockpile of proteins for the first 12 cell divisions (12). Furthermore, the accuracy of our H1/N estimation is reduced by the variation in the amount of DNA injected into each individual oocyte (see Materials and Methods). Hence, we propose that the H1-induced effect on the NRL can be used to quantify the level of H1 expression required to saturate the chromatin with one entity of H1 per nucleosome, i.e., an apparent H1/N ratio of 1.6 to 2 in our experimental setup (Fig. 4B).

Mechanism of H1-enhanced GR binding. Our results imply that the mechanism of H1-enhanced GR binding is a direct result of two separate H1-dependent phenomena, i.e., the H1 concentration-dependent transition in the higher-order chromatin structure (Fig. 8) and the GR-induced dissociation of H1 from the active chromatin domain (Fig. 7). These findings converge into the following mechanism. Hormone-induced GR scans the accessible DNA and eventually forms specific GRE contacts, leading to the recruitment of coactivators. The activity of these putative coactivators, e.g., chromatin remodeling and/or histone modifications, leads to a local dissociation of H1 (Fig. 7). Thus, a new equilibrium in H1 binding is established, where H1 remains bound to and partially shields the DNA linkers of the bulk chromatin, while the H1 concentration at the active chromatin domains is drastically reduced, which contributes to the formation of more accessible DNA in the activated domain. A reduced fraction of GR is thus occupied in the inactive chromatin, which increases the free GR pool and enhances GR binding to the specific GREs located in the activated and H1-depleted chromatin domain (Fig. 9). The reasons for a maximal effect to occur at a subsaturating level of H1 may be several. At higher levels, H1 may tend to reoccupy the chromatin sites from which it was dissociated. Alternatively, a subsaturating H1 level may enhance the chromatin dynamics by frequent switching of each nucleosome between the bound H1 and the free state, or a subsaturating level of H1 may induce a particular higher-order chromatin structure that more efficiently shields the nonspecific DNA. The latter alternative is supported by the experiment for which results are shown in Fig. 8, showing that DNA digestion by MNase is reduced at the same subsaturating level of H1 that stimulates GR binding. The structure of this H1-induced chromatin is enigmatic, but a reasonable assumption is that it requires a particular concentration of H1 (Fig. 8).

Can the H1-stimulated GR binding be due to the H1-induced difference in nucleosome density since H1-binding increases the NRL, in our case from 164 to 173 bp? This is not likely to be the case for the following reason. We have failed to detect any effect of H1 on GR binding or MMTV transcription at early time points of hormone induction (data not shown). On the contrary, we can only detect the H1-stimulated GR binding at equilibrium of the hormone-activated state, i.e., when the H1 has been dissociated from chromatin. In this situation, the NRL is the same in the active chromatin domain

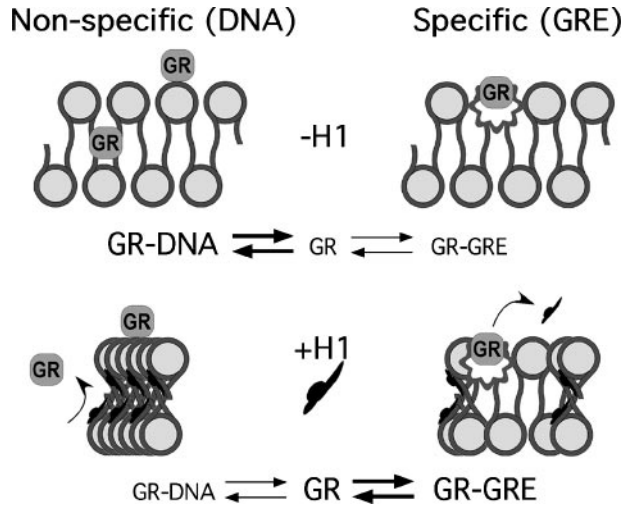

FIG. 9. The proposed mechanism of H1-enhanced binding of GR to the GRE in vivo. Hormone-activated GR induces a selective dissociation of H1 from the active chromatin domain. An asymmetric H1 equilibrium is formed that selectively reduces the DNA access in the inactive chromatin domain. This reduces the amount of GR that is occupied by searching through the nonspecific DNA and hence increases the free GR pool that is available for interaction with the GRE.

irrespective of the presence or absence of H1 (Fig. 7B, upper panels).

Recent results suggest that the cellular content of H1 is less than one per nucleosome and that different cell types vary in H1 content from an ~0.5 H1/N ratio in embryonic stem cells to a 0.83 H1/N ratio in thymocytes (see reference 47 for a review). Our results demonstrate a functional consequence of maintaining a subsaturating concentration of H1, i.e., an optimized protein-DNA binding for a gene-specific transcription factor. We propose that this is the functional rationale for the maintenance of substoichiometric levels of H1/N in different cell types (47).

Dissociation of H1 during chromatin activation. The actively transcribed MMTV promoter is depleted of histone H1 (11, 23, 28) (Fig. 7). As discussed above, the hormone-activated GR remodels the local chromatin to form the more open and H1-free state. However, we note that H1 is still present at the MMTV promoter together with constitutively bound NF1 and Oct1. Coexpression of NF1 and Oct1 was shown to alter the MMTV LTR chromatin structure into a preset state (8) and to enhance basal MMTV transcription (5). Taken together, this implies that the dissociation of histone H1 is dependent on the recruitment of a certain threshold of chromatin-remodeling activity and/or histone-modifying activity. In our system, this task is accomplished by GR rather than by NF1 and Oct1 (8). Importantly, GR binding to DNA in the absence of NF1 and Oct1 is also enhanced by H1 (Fig. 3B). We and others have shown that NF1 and Oct1 binding at the hormone-activated MMTV promoter are cooperative events mediated by GR binding in vivo (8, 44) and that NF1 is bound with ~50-fold-higher affinity to the GR-activated MMTV promoter than to the inactive promoter (5). This may suggest that the H1-stimulated binding of all three factors is mediated by GR alone, and thus, the enhanced NF1 and Oct1 binding is a cooperative effect of GR binding. This cooperative effect may be due to direct protein-protein contact, structural remodeling of the nucleosomal DNA (46), and/or locally stabilizing effects of GR-mediated dissociation of H1. The lack of H1 enhancement of the constitutive NF1 binding (Fig. 3C) and Oct1 binding (data not shown) corroborates our GR-induced H1 asymmetric distribution model (Fig. 9), since H1 is not dissociated from the promoter by NF1 and Oct1 (Fig. 7A and Åstrand et al., unpublished).

The removal of histone H1 in *Tetrahymena* (39) and the reduction of H1 content in mice (19, 20) lead to variable effects on the expression of a subset of genes. Our results suggest these effects to be at least partly caused by the loss of the H1 concentration-dependent enhancement in DNA binding of gene-specific transcription factors. Here we show that this is the case for GR induction. However, based on the proposed mechanism (Fig. 9), we expect H1 to mediate similar effects on many, if not all, sequence-specific DNA binding factors that are able to initiate local dissociation of H1 from the activated chromatin domain. The outcome of the H1 reduction or loss may vary for each gene, depending on its requirement of different combinations of activators and/or repressors. Based on our results, we propose that the essential role of H1 in mouse development, demonstrated by deletion of three of five somatic H1 genes (19, 20), is due to a global imbalance in gene expression caused by the loss of the H1-mediated effect. Our model predicts that this would affect the expression pattern of most of the genes but to a variable extent and often to such a low extent that the effect is difficult to detect by cDNA array analysis. The cutoff level for a significant effect on such an expression analysis is often chosen to be at twofold (20), and this may already exceed the subtle effect of a reduced H1 level.

Others have reported that an H1/N level slightly above 1 in in vitro-assembled chromatin corrupts both the in vitro transcription and the organization of a nucleosome array (21, 25). In our in vivo experiments, even very high levels of H1 did not completely stop hormone-induced transcription (Fig. 5B), although it was reduced, while the stimulatory effect of H1 on transcription and GR binding required a subsaturating level of H1/N (Fig. 5). Our topology experiments show that there is no significant loss in negative DNA supercoiling until the H1/N ratio is ~2.6 (Fig. 2E) in spite of the increase in NRL of ~9 to 12 bp seen already at an ~1.6 H1/N ratio (Fig. 2C and 4B). The increased NRL is expected to cause a loss of 2 to 3 nucleosomes from the 7,249-bp M13 template and, hence, to result in the loss of 2 to 3 negative supercoils. However, binding of linker histone to the nucleosome enhances its ability to accommodate both negative and positive changes in the topology via the H1-induced formation of a DNA stem that is then able to rotate in either direction along its longitudinal axis (41). Such an H1-induced stem formation, perhaps in combination with an altered helical setting of the DNA around the chromatosome, may explain the lack of a topological effect in our in vivo experiments until we reach a certain level of H1, i.e., an H1/N ratio of ~2.6. Such an oversaturating amount of H1 results in aberrant H1 binding, as illustrated by the ChIP experiments (see Supplement S3 in the supplemental material) where strong reduction of HA-H1 cross-linking was seen at a wt H1 competitor concentration resulting in an ~1.7 H1/N ratio, and then a gradually increased cross-linking of HA-H1 occurred at

the higher competitor levels of H1/N ratios of ~2.6 to 3.5. This indicates that H1, after saturating its high-affinity nucleosomal site, starts to occupy low-affinity DNA sites, which leads to structural effects detected as a loss of negative supercoils (Fig. 2D and E) and a corrupted chromatin structure (Fig. 2B). We assume that this is caused by nonspecific electrostatic interaction between H1 and DNA. However, our results demonstrate that this nonspecific H1 binding does not occur within the physiological concentration of H1, i.e., the substoichiometric level of H1 in relation to nucleosomes.

In conclusion, our work shows that H1 binds to a specific and saturable site in in vivo-assembled chromatin, that H1 enhances GR-DNA binding in vivo, and that this enhancement is strictly H1 concentration dependent and occurs at a substoichiometric level of H1 in relation to the nucleosomes. The H1-dependent reduction of DNA access (Fig. 8) and the GR-induced dissociation of H1 from active chromatin (Fig. 7) suggest that the mechanism of H1-enhanced GR binding is caused by the GR-induced asymmetric distribution of H1 in active versus inactive chromatin (Fig. 9). Our results provide a functional rationale for the previously reported finding that most cells contain a substoichiometric level of H1 in relation to nucleosomes (47). Furthermore, the saturable binding of H1 to chromatin in vivo (Fig. 2 and 4) raises the question of whether core histone modifications and/or linker histone modifications, different H1 subtypes, and/or the presence of other chromatin-associated proteins, such as HP1 (17) or TopoIIβ and poly-(ADP-ribose) polymerase 1 (27), can regulate linker histone affinity for its binding to individual nucleosomes or different cellular states and thereby adjust the local or global chromatin structure for various cellular activities (36).

ACKNOWLEDGMENTS

This work was supported by grants to Ö.W. and S.B. from the Swedish Cancer Foundation (project 2222-B05-21XBB), to Ö.W. from the Medical Research Council (31BI-15338-01A), to Ö.W. from the Knut and Alice Wallenberg Foundation, and to S.B. from the Medical Research Council (project K2006-31X-20075-01-3). Ö.W. is an associate member of the EU NoE, The Epigenome.

We are grateful to Kiyoe Ura for a great deal of encouragement and support and for kindly providing cDNAs for xB4, and we are grateful to Ohsumi Keita for the generous gift of xB4 antiserum and the xH1A cDNA. We also thank Qiao Li and Ulla Björk for the construction of pGo2.5Go-39MTV:M13, and we are grateful to Per-Henrik Holmqvist for helpful discussions and support during this work.

REFERENCES

1. **Almouzni, G., and A. P. Wolffe.** 1993. Replication-coupled chromatin assembly is required for repression of basal transcription *in vivo*. Genes Dev. **7:**2033–2047.
2. **Astrand, C., T. Klenka, O. Wrange, and S. Belikov.** 2004. Trichostatin A reduces hormone-induced transcription of the MMTV promoter and has pleiotropic effects on its chromatin structure. Eur. J. Biochem. **271:**1153–1162.
3. **Bates, D. L., and J. O. Thomas.** 1981. Histones H1 and H5: one or two molecules per nucleosome? Nucleic Acids Res. **9:**5883–5894.
4. **Becker, P. B., and W. Horz.** 2002. ATP-dependent nucleosome remodeling. Annu. Rev. Biochem. **71:**247–273.
5. **Belikov, S., C. Astrand, P. H. Holmqvist, and O. Wrange.** 2004. Chromatin-mediated restriction of nuclear factor 1/CTF binding in a repressed and hormone-activated promoter in vivo. Mol. Cell. Biol. **24:**3036–3047.
6. **Belikov, S., B. Gelius, G. Almouzni, and Ö. Wrange.** 2000. Hormone activation induces nucleosome positioning *in vivo*. EMBO J. **19:**1023–1033.
7. **Belikov, S., B. Gelius, and O. Wrange.** 2001. Hormone-induced nucleosome positioning in the MMTV promoter is reversible. EMBO J. **20:**2802–2811.
8. **Belikov, S., P. H. Holmqvist, C. Astrand, and O. Wrange.** 2004. Nuclear factor 1 and octamer transcription factor 1 binding preset the chromatin structure of the mouse mammary tumor virus promoter for hormone induction. J. Biol. Chem. **279:**49857–49867.
9. **Bellard, M., G. Dretzen, A. Giangrande, and P. Ramain.** 1989. Nuclease digestion of transcriptionally active chromatin. Methods Enzymol. **170:**317–346.
10. **Bhattacharjee, R. N., G. C. Banks, K. W. Trotter, H. L. Lee, and T. K. Archer.** 2001. Histone H1 phosphorylation by Cdk2 selectively modulates mouse mammary tumor virus transcription through chromatin remodeling. Mol. Cell. Biol. **21:**5417–5425.
11. **Bresnick, E. H., M. Bustin, V. Marsaud, H. Richard-Foy, and G. L. Hager.** 1992. The transcriptionally-active MMTV promoter is depleted of histone H1. Nucleic Acids Res. **20:**273–278.
12. **Brown, D. D.** 2004. A tribute to the Xenopus laevis oocyte and egg. J. Biol. Chem. **279:**45291–45299.
13. **Brown, D. T.** 2003. Histone H1 and the dynamic regulation of chromatin function. Biochem. Cell Biol. **81:**221–227.
14. **Brown, D. T., T. Izard, and T. Misteli.** 2006. Mapping the interaction surface of linker histone H1(0) with the nucleosome of native chromatin in vivo. Nat. Struct. Mol. Biol. **13:**250–255.
15. **Buetti, E., and B. Kuhnel.** 1986. Distinct sequence elements involved in the glucocorticoid regulation of the mouse mammary tumor virus promoter identified by linker scanning mutagenesis. J. Mol. Biol. **190:**379–389.
16. **Catez, F., T. Ueda, and M. Bustin.** 2006. Determinants of histone H1 mobility and chromatin binding in living cells. Nat. Struct. Mol. Biol. **13:**305–310.
17. **Daujat, S., U. Zeissler, T. Waldmann, N. Happel, and R. Schneider.** 2005. HP1 binds specifically to Lys26-methylated histone H1.4, whereas simultaneous Ser27 phosphorylation blocks HP1 binding. J. Biol. Chem. **280:**38090–38095.
18. **Dimitrov, S., G. Almouzni, M. Dasso, and A. P. Wolffe.** 1993. Chromatin transitions during early Xenopus embryogenesis: changes in histone H4 acetylation and in linker histone type. Dev. Biol. (Orlando) **160:**214–227.
19. **Fan, Y., T. Nikitina, E. M. Morin-Kensicki, J. Zhao, T. R. Magnuson, C. L. Woodcock, and A. I. Skoultchi.** 2003. H1 linker histones are essential for mouse development and affect nucleosome spacing in vivo. Mol. Cell. Biol. **23:**4559–4572.
20. **Fan, Y., T. Nikitina, J. Zhao, T. J. Fleury, R. Bhattacharyya, E. E. Bouhassira, A. Stein, C. L. Woodcock, and A. I. Skoultchi.** 2005. Histone H1 depletion in mammals alters global chromatin structure but causes specific changes in gene regulation. Cell **123:**1199–1212.
21. **Fyodorov, D. V., and J. T. Kadonaga.** 2003. Chromatin assembly in vitro with purified recombinant ACF and NAP-1. Methods Enzymol. **371:**499–515.
22. **Gelius, B., P. Wade, A. P. Wolffe, Ö. Wrange, and A.-K. Östlund Farrants.** 1999. Characterization of a chromatin remodeling activity in *Xenopus* oocytes. Eur. J. Biochem. **262:**426–434.
23. **Georgel, P. T., T. M. Fletcher, G. L. Hager, and J. C. Hansen.** 2003. Formation of higher-order secondary and tertiary chromatin structures by genomic mouse mammary tumor virus promoters. Genes Dev. **17:**1617–1629.
24. **Gunjan, A., and D. T. Brown.** 1999. Overproduction of histone H1 variants in vivo increases basal and induced activity of the mouse mammary tumor virus promoter. Nucleic Acids Res. **27:**3355–3363.
25. **Hansen, J. C.** 2002. Conformational dynamics of the chromatin fiber in solution: determinants, mechanisms, and functions. Annu. Rev. Biophys. Biomol. Struct. **31:**361–392.
26. **Huynh, V. A., P. J. Robinson, and D. Rhodes.** 2005. A method for the in vitro reconstitution of a defined "30 nm" chromatin fibre containing stoichiometric amounts of the linker histone. J. Mol. Biol. **345:**957–968.
27. **Ju, B. G., V. V. Lunyak, V. Perissi, I. Garcia-Bassets, D. W. Rose, C. K. Glass, and M. G. Rosenfeld.** 2006. A topoisomerase IIbeta-mediated dsDNA break required for regulated transcription. Science **312:**1798–1802.
28. **Koop, R., L. Di Croce, and M. Beato.** 2003. Histone H1 enhances synergistic activation of the MMTV promoter in chromatin. EMBO J. **22:**588–599.
29. **Laybourn, P. J., and J. T. Kadonaga.** 1991. Role of nucleosomal cores and histone H1 in regulation of transcription by RNA polymerase II. Science **254:**238–245.
30. **Lever, M. A., J. P. Th'ng, X. Sun, and M. J. Hendzel.** 2000. Rapid exchange of histone H1.1 on chromatin in living human cells. Nature **408:**873–876.
31. **Li, Q., and Ö. Wrange.** 1995. Accessibility of a glucocorticoid response element in a nucleosome depends on its rotational positioning. Mol. Cell. Biol. **15:**4375–4384.
32. **McKnight, S. L., and R. Kingsbury.** 1982. Transcriptional control signals of a eukaryotic protein-coding gene. Science **217:**316–324.
33. **Misteli, T., A. Gunjan, R. Hock, M. Bustin, and D. T. Brown.** 2000. Dynamic binding of histone H1 to chromatin in living cells. Nature **408:**877–881.
34. **Nightingale, K. P., D. Pruss, and A. P. Wolffe.** 1996. A single high affinity binding site for histone H1 in a nucleosome containing the Xenopus borealis 5 S ribosomal RNA gene. J. Biol. Chem. **271:**7090–7094.
35. **Richard-Foy, H., and G. L. Hager.** 1987. Sequence-specific positioning of nucleosomes over the steroid-inducible MMTV promoter. EMBO J. **6:**2321–2328.
36. **Robinson, P. J., and D. Rhodes.** 2006. Structure of the '30 nm' chromatin fibre: a key role for the linker histone. Curr. Opin. Struct. Biol. **16:**336–343.

37. **Saeki, H., K. Ohsumi, H. Aihara, T. Ito, S. Hirose, K. Ura, and Y. Kaneda.** 2005. Linker histone variants control chromatin dynamics during early embryogenesis. Proc. Natl. Acad. Sci. USA **102:**5697–5702.
38. **Segalla, S., L. Rinaldi, C. Kilstrup-Nielsen, G. Badaracco, S. Minucci, P. G. Pelicci, and N. Landsberger.** 2003. Retinoic acid receptor alpha fusion to PML affects its transcriptional and chromatin-remodeling properties. Mol. Cell. Biol. **23:**8795–8808.
39. **Shen, X., and M. A. Gorovsky.** 1996. Linker histone H1 regulates specific gene expression but not global transcription in vivo. Cell **86:**475–483.
40. **Shrader, T. E., and D. M. Crothers.** 1989. Artificial nucleosome positioning sequences. Proc. Natl. Acad. Sci. USA **86:**7418–7422.
41. **Sivolob, A., and A. Prunell.** 2003. Linker histone-dependent organization and dynamics of nucleosome entry/exit DNAs. J. Mol. Biol. **331:**1025–1040.
42. **Tanaka, M., J. D. Hennebold, J. Macfarlane, and E. Y. Adashi.** 2001. A mammalian oocyte-specific linker histone gene H1oo: homology with the genes for the oocyte-specific cleavage stage histone (cs-H1) of sea urchin and the B4/H1M histone of the frog. Development **128:**655–664.
43. **Thomas, J. O.** 1999. Histone H1: location and role. Curr. Opin. Cell Biol. **11:**312–317.
44. **Truss, M., J. Bartsch, A. Schulbert, R. J. G. Hache, and M. Beato.** 1995. Hormone induces binding of receptors and transcription factors to a rearranged nucleosome on the MMTV promoter in vivo. EMBO J. **14:**1737–1751.
45. **Ura, K., J. J. Hayes, and A. P. Wolffe.** 1995. A positive role for nucleosome mobility in the transcriptional activity of chromatin templates: restriction by linker histones. EMBO J. **14:**3752–3765.
46. **Vicent, G. P., A. S. Nacht, C. L. Smith, C. L. Peterson, S. Dimitrov, and M. Beato.** 2004. DNA instructed displacement of histones H2A and H2B at an inducible promoter. Mol. Cell **16:**439–452.
47. **Woodcock, C. L., A. I. Skoultchi, and Y. Fan.** 2006. Role of linker histone in chromatin structure and function: H1 stoichiometry and nucleosome repeat length. Chromosome Res. **14:**17–25.
48. **Zhou, Y. B., S. E. Gerchman, V. Ramakrishnan, A. Travers, and S. Muyldermans.** 1998. Position and orientation of the globular domain of linker histone H5 on the nucleosome. Nature **395:**402–405.

MOLECULAR AND CELLULAR BIOLOGY, Nov. 2008, p. 6730 Vol. 28, No. 21
0270-7306/08/$08.00+0 doi:10.1128/MCB.01333-08

AUTHOR'S CORRECTION

Mechanism of Histone H1-Stimulated Glucocorticoid Receptor DNA Binding In Vivo

Sergey Belikov, Carolina Åstrand, and Örjan Wrange

Department of Cell and Molecular Biology, Karolinska Institutet, SE-17177 Stockholm, Sweden

Volume 27, no. 6, p. 2398–2410, 2007. The subtype of linker histone H1 primarily used in this work was *Xenopus* H1o (xH1o) and not *Xenopus* H1A (xH1A) as was erroneously stated in the report. We sincerely apologize for this error; however, it does not affect the conclusions on the mechanism of linker histone H1-stimulated glucocorticoid receptor binding made in this work since we find the same qualitative effects of xH1A as shown to occur with xH1o. Specifically, experiments demonstrated in Fig. 1 to 5, 7B, and 8 and Supplement S1 in the supplemental material were conducted with xH1o; however, the chromatin immunoprecipitation experiments in Fig. 6C and 7A and Supplements S2 and S3 in the supplemental material were indeed done with an N-terminally hemagglutinin (HA)-tagged xH1A construct. The experiment in Supplement S3 in the supplemental material demonstrates that wild-type H1o and HA-H1A compete for the same binding site in chromatin. This argues that the effects are general linker histone effects.

The estimation of the H1/nucleosome (H1/N) ratio was based on the incorporation of [^{14}C]lysine after mRNA injection; since xH1o harbors 54 lysine residues while xH1A has 64 lysine residues, the H1/N ratios should be 19% higher than indicated (~1.19-fold higher) in Fig. 1 to 5 and 8 and Supplements S1 and S3 in the supplemental material. This is within the error of this semiquantitative estimation.

Page 2398, abstract, line 3: "H1A" should read "H1o."

Page 2399, column 1, line 18: "H1A" should read "H1o."

Page 2399, column 1, Materials and Methods, line 6: "...DQ466082), and..." should read "...DQ466082), plasmids for production of mRNA for histone H1 were from a PCR-amplified xH1 cDNA clone (kindly provided by K. Ura, accession number Z71503), and...."

Page 2399, Fig. 1B: "H1A" should read "H1" in both places.

Page 2399, legend to Fig. 1, lines 5, 8, and 11: "H1A" should read "H1."

Page 2400, column 1, line 14: "HA-H1A, dubbed HA-H1, was" should read ″HA-H1A was."

Page 2405, column 1, lines 35, 36 (twice), 39, 43 (twice), 44, 51, and 57: ″H1" should read "H1A."

Page 2405, column 2, lines 4 and 7: "H1" should read "H1A."

Page 2405, legend to Fig. 6, line 4 from bottom: "HA-H1 mRNA" should read "HA-H1A mRNA (HA-H1)."

Page 2406, legend to Fig. 7, line 1: "H1" should read "H1A."

Page 2406, legend to Fig. 7, line 3: "HA-H1 mRNA" should read "HA-H1A mRNA (HA-H1)."

Page 2406, column 2, lines 1 and 3: "H1" should read "H1A."

Page 2408, column 2, lines 3 and 1 from bottom: ″H1" should read "H1A."

Revised supplemental material, in which the H1 labeling in Supplements S2 and S3 is corrected, is posted at http://mcb.asm.org/cgi/content/full/27/6/2398/DC1.